COOPERATIVE SIMULTANEOUS LOCALIZATION AND TRACKING FOR MOBILE AD-HOC SENSOR NETWORKS

Jing Teng, Rong Zhou, Ying Zhang*

School of Control and Computer Engineering
North China Electric Power University
102206 Beijing, China
email: jing.teng@ncepu.edu.cn*, zhourong@ncepu.edu.cn, yingzhang@ncepu.edu.cn

ABSTRACT

Over the past decade, there has been much focus on mobile ad-hoc sensor networks. The mobility alleviates several issues relating to sensor network coverage and connectivity, whereas aggravates the difficulties of applications such as target tracking. Traditional solutions always localize the sensors first, and then track the target. In contrast, cooperative simultaneous localization and tracking (CoSLAT) adopts both the sensor-target and the inter-sensor observations to simultaneously refine the target and the sensor estimates. We propose a distributed variational filtering (VF) algorithm for CoSLAT, which greatly cuts down the estimate errors, while having nearly the same complexity as the traditional particle filtering (PF) algorithm. In addition, the update and the approximation of the $a\ posteriori$ distribution are jointly performed by the VF, yielding a natural and adaptive compression. Since the temporal dependence is reduced from a great number of particles to one Gaussian component, the communication cost is significantly diminished.

Index Terms— Variational Filtering; Cooperative Simultaneous Localization and Tracking; Mobile Ad-hoc sensor NETworks

1. INTRODUCTION

Mobile Ad-hoc sensor NETworks (MANETs) are a particular class of wireless sensor networks (WSN), in which mobility plays a key role. The mobility endows MANETs with significant advantages, such as low-cost, easy-deployment, self-management and no requirement for established infrastructure etc., compared with the traditional way of manual deployment or the expensive way of GPS receiver equipping [1–3]. The dominant inference tasks of WSN include sensor localization (SL) and target tracking (TT) [4, 5], where TT requires the sensor positions known $a\ priori$. Therefore, traditional solutions first localize the mobile sensors, then these estimated sensor locations, along with the sensor-target observations, are used for TT. However, the first localization then tracking (FLTT) approach is sub-optimal, since the sensor-target observations are not used to refine the sensor positions [6]. Particularly in the case of MANETs, the mobility of the sensors emphasizes the online update of sensor locations. In contrast to the FLTT approach, simultaneous localization and tracking (SLAT) [7], applies the sensor-target observations to track a target while simultaneously localizing the static sensors. However, the SLAT algorithm needs to be executed centralized, due to the significantly higher complexity than FLTT. Meyer [5] introduced a framework of cooperative SLAT (CoSLAT), which extends the SLAT by using inter-sensor measurements, thus could be adopted to MANETs. Unfortunately, the proposed CoSLAT algorithm suffers from high computation and communication costs due to the particle-based message representation. Therefore, they proposed an advanced hybrid particle-based and parametric message passing algorithm for CoSLAT in [8], where a Gaussian Mixture Model (GMM) was adopted to approximate the marginal posterior distribution, leading to a reduction of the belief propagation. On the contrary, the propagation of inference errors is unavoidable, due to the approximation of the marginal posterior distribution. In this paper, we employ the variational method in the place of mixture gaussian model to approximate the joint state during the measurement incorporation phase, avoiding description complexity and unnecessary communication. Since the approximation phase is jointly performed with the update phase of the $a\ posteriori$ distribution [9], the generally inevitable error propagation problem is terminated.

The remainder of this paper is organized as follows. In Section 2, the system models are defined. The variational filtering algorithm for CoSLAT in MANETs is described in detailIn Section 3. The performance of the proposed algorithm is evaluated through the simulations in Section 4. Section 5 concludes this paper.

Supported by the Fundamental Research Funds for the Central Universities, Specialized Research Fund for the Doctoral Program of Higher Education (No.20130036120003), National Natural Science Foundation of China (No.61305056)

978-0-9928626-3-3/15/$31.00 ©2015 IEEE

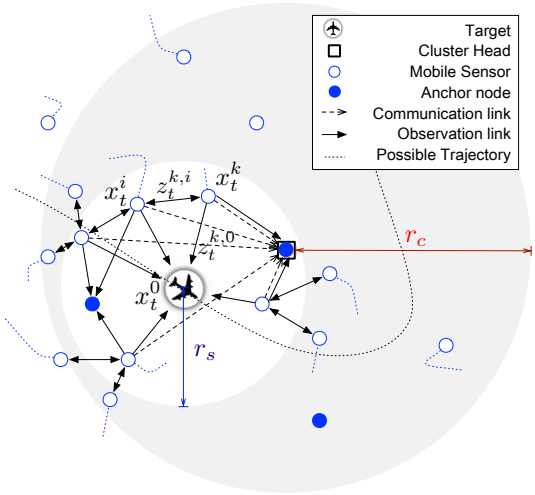

Fig. 1: Example of a MANET with a target traveling through.

2. SYSTEM MODELS

In this study, we consider a MANET consisting of N_s mobile sensors and a small subset of N_a anchor nodes (i.e., static sensors with perfect location information), where one passive target travels through, as depicted in Fig. 1. The mobile nodes (including both the mobile sensors and the target to track) are moving arbitrarily, where changes in direction and speed occur uncontrollably. A Random Walk Mobility (RWM) model [10], which mimics an erratic movement of a mobile node in extremely unpredictable situations, was employed in our simulations.

In order to minimize energy and bandwidth consumption, the proposed algorithm is distributively executed on a cluster base. Only the sensors that detect the target form an activated cluster to perform signal processing, as denoted by the white disc with the center $\boldsymbol{x}_t^0$ and the radius r_s in Fig. 1. The communication range is defined as twice of the sensing range ($r_c = 2r_s$), which guarantees that one and only one cluster is formed at each instant, and the communication in the activated cluster is within one-hop. The anchor node within the activated cluster works as the cluster head (CH). In the case of multiple anchors in a cluster, the one with the maximum residual energy is elected as the CH. The other slave sensors then transfer their observations of the target (e.g. $z_t^{k,0}$) to the CH, which are incorporated to update the target temporal estimation. The inter-sensor observations (e.g. $z_t^{k,i}$) are combined with the sensor-target observation to perform self-localization algorithm in each slaver locally. For the sake of clarity, we index the mobile node by a superscript k, where $\boldsymbol{x}_t^0$ designates the target, and $\boldsymbol{x}_t^{k\neq 0}$ denotes the mobile sensor node. According to the classical Bayesian filtering framework, the objective distribution of interest takes the form of *a posteriori* distribution $p(\boldsymbol{x}_t^k|\boldsymbol{z}_{1:t}^k)$, which could be calculated by:

$$p(\boldsymbol{x}_t^k|\boldsymbol{z}_{1:t}^k) = \frac{p(\boldsymbol{z}_t^k|\boldsymbol{x}_t^k)p(\boldsymbol{x}_t^k|\boldsymbol{z}_{1:t-1}^k)}{p(\boldsymbol{z}_t^k|\boldsymbol{z}_{1:t-1}^k)}, \quad (1)$$

$$\text{where} \quad p(\boldsymbol{z}_t^k|\boldsymbol{z}_{1:t-1}^k) = \int p(\boldsymbol{z}_t^k|\boldsymbol{x}_t^k)p(\boldsymbol{x}_t^k|\boldsymbol{z}_{1;t-1}^k)d\boldsymbol{x}_t^k,$$

$$p(\boldsymbol{x}_t^k|\boldsymbol{z}_{1:t-1}^k) = \int p(\boldsymbol{x}_t^k|\boldsymbol{x}_{t-1}^k)p(\boldsymbol{x}_{t-1}^k|\boldsymbol{z}_{1:t-1}^k)d\boldsymbol{x}_{t-1}^k. \quad (2)$$

In Eq. (1), an observation model $p(\boldsymbol{z}_t^k|\boldsymbol{x}_t^k)$ is incorporated to update the prediction $p(\boldsymbol{x}_t^k|\boldsymbol{z}_{1:t-1}^k)$, in order to arrive at a new and hopefully more accurate state estimate. The prediction phase uses the state estimate from the previous sampling instant, namely $p(\boldsymbol{x}_{t-1}^k|\boldsymbol{z}_{1:t-1}^k)$, together with a state evolution model $p(\boldsymbol{x}_t^k|\boldsymbol{x}_{t-1}^k)$ to produce a prediction $p(\boldsymbol{x}_t^k|\boldsymbol{z}_{1:t-1}^k)$ according to Eq. (2). Recursive computation of the two equations allows online update of the mobile state estimation, where the definitions of $p(\boldsymbol{x}_t^k|\boldsymbol{x}_{t-1}^k)$ and $p(\boldsymbol{z}_t^k|\boldsymbol{x}_t^k)$ are of great importances.

2.1. General State Evolution Model

Since the target and the mobile nodes travels arbitrarily in the sensor field, we employ a General State Evolution Model (GSEM). This model is more appropriate to practical nonlinear and non-Gaussian situations, with no *a priori* information on the velocity or the acceleration. The temporal position $\boldsymbol{x}_t^k$ is assumed to follow a Gaussian model, where the expectation $\boldsymbol{\mu}_t^k$ and the precision matrix $\boldsymbol{\lambda}_t^k$ are both random. The randomness of the expectation and the precision is used here to further capture the uncertainty of the state distribution. A practical choice of these distributions is a Gaussian distribution for the expectation $\boldsymbol{\mu}_t^k$ and a Wishart distribution for the precision matrix $\boldsymbol{\lambda}_t^k$. In other words, the hidden state $\boldsymbol{x}_t^k$ is extended to $\boldsymbol{\alpha}_t^k = (\boldsymbol{x}_t^k, \boldsymbol{\mu}_t^k, \boldsymbol{\lambda}_t^k)$, yielding a hierarchical model as follows,

$$\begin{cases} \boldsymbol{x}_t^k & \sim & \mathcal{N}(\boldsymbol{x}_t^k|\boldsymbol{\mu}_t^k, \boldsymbol{\lambda}_t^k) \\ \boldsymbol{\mu}_t^k & \sim & \mathcal{N}(\boldsymbol{\mu}_t^k|\boldsymbol{\mu}_{t-1}^k, \bar{\boldsymbol{\lambda}}^k) \\ \boldsymbol{\lambda}_t^k & \sim & \mathcal{W}_d(\boldsymbol{\lambda}_t^k|\bar{\boldsymbol{V}}^k, \bar{n}^k) \end{cases}. \quad (3)$$

The denotation $\bar{\cdot}$ represents the fixed hyper-parameter, where $\bar{\boldsymbol{\lambda}}^k$, $\bar{n}^k$ and $\bar{\boldsymbol{V}}^k$ are the random walk precision matrix, the degrees of freedom and the precision of the Wishart distribution, respectively. The dimension the Wishart distribution equals to that of the mobile node state ($d = 2$), whereas an extension to the 3D case is straightforward.

Assuming a random mean and a random covariance for the state $\boldsymbol{x}_t^k$ leads to a probability distribution covering a wide range of tail behaviors, which allows discrete jumps in the mobile node trajectory. The marginal state distribution is obtained by integrating over the mean and precision matrix as

follows,

$$p(\boldsymbol{x}_t^k|\boldsymbol{x}_{t-1}^k) = \int\int \mathcal{N}(\boldsymbol{x}_t^k|\boldsymbol{\mu}_t^k, \boldsymbol{\lambda}_t^k) p(\boldsymbol{\mu}_t^k, \boldsymbol{\lambda}_t^k|\boldsymbol{x}_{t-1}^k) d\boldsymbol{\mu}_t^k d\boldsymbol{\lambda}_t^k. \tag{4}$$

2.2. Observation Model

Take the mobile sensor $\boldsymbol{x}_t^k, (k \neq 0)$ for example, its observation of the mobile node $\boldsymbol{x}_t^i, (i \neq k)$, which could be either the target ($i = 0$) or other mobile sensor node ($i \neq 0$) , is modeled as

$$z_t^{k,i} = \begin{cases} \parallel \boldsymbol{x}_t^k - \boldsymbol{x}_t^i \parallel + \varepsilon_k, & \text{if } \parallel \boldsymbol{x}_t^k - \boldsymbol{x}_t^i \parallel \leqslant r_s \\ 0, & \text{otherwise} \end{cases}, \tag{5}$$
$$\text{with} \quad \varepsilon_k \sim \mathcal{N}(0, \sigma_k^2).$$

The measurement noise ε_k is assumed to be independent for each detecting sensor $\boldsymbol{x}_t^k$.

3. PROPOSED METHOD

With the definition of the GSEM in the section 2.1 and the observation model in the section 2.2, the inference problem can be reduced to calculation of integrals in Eq. (1). However, the hidden state $\boldsymbol{x}_t^k$ to be estimated is extended to $\boldsymbol{\alpha}_t^k$ by the GSEM, resulting an augmented $a\ posteriori$ distribution $p(\boldsymbol{\alpha}_t^k|\boldsymbol{z}_{1:t}^k)$. In addition, the non-linear and non-Gaussian aspects in Eq. (3) lead to intractable integrals. Therefore, we propose a Variational Filtering (VF) approach to approximate $p(\boldsymbol{\alpha}_t^k|\boldsymbol{z}_{1:t}^k)$ by a separable distribution $q(\boldsymbol{\alpha}_t^k)$, while minimizing the Kullback-Leibler (KL) divergence error:

$$\begin{aligned} D_{\mathrm{KL}}(q||p) &= \int q(\boldsymbol{\alpha}_t^k) \log \frac{q(\boldsymbol{\alpha}_t^k)}{p(\boldsymbol{\alpha}_t^k|\boldsymbol{z}_{1:t}^k)} (d\boldsymbol{\alpha}_t^k), \\ \text{where} \quad q(\boldsymbol{\alpha}_t^k) &= q(\boldsymbol{x}_t^k) q(\boldsymbol{\mu}_t^k) q(\boldsymbol{\lambda}_t^k). \end{aligned} \tag{6}$$

Accordingly $p(\boldsymbol{\alpha}_t^k|\boldsymbol{z}_{1:t}^k)$is deduced to,

$$\begin{aligned} \hat{p}(\boldsymbol{\alpha}_t^k|\boldsymbol{z}_{1:t}^k) &= \frac{p(\boldsymbol{z}_t|\boldsymbol{\alpha}_t^k) \int p(\boldsymbol{\alpha}_t^k|\boldsymbol{\alpha}_{t-1}^k) q(\boldsymbol{\alpha}_{t-1}^k) d\boldsymbol{\alpha}_{t-1}^k}{p(\boldsymbol{z}_t^k|\boldsymbol{z}_{1:t-1}^k)} \\ &\propto p(\boldsymbol{z}_t^k|\boldsymbol{x}_t^k) p(\boldsymbol{x}_t^k|\boldsymbol{\mu}_t^k, \boldsymbol{\lambda}_t^k) p(\boldsymbol{\lambda}_t^k) q_p(\boldsymbol{\mu}_t^k), \\ \text{where} \quad q_p(\boldsymbol{\mu}_t^k) &= \int p(\boldsymbol{\mu}_t^k|\boldsymbol{\mu}_{t-1}^k) q(\boldsymbol{\mu}_{t-1}^k) d\boldsymbol{\mu}_{t-1}^k. \end{aligned} \tag{7}$$

With variational calculus, the following approximate distribution is yielded,

$$\begin{cases} q(\boldsymbol{x}_t^k) \propto \exp\langle \log\ p(\boldsymbol{z}_{1:t}^k, \boldsymbol{\alpha}_t)\rangle_{q(\boldsymbol{\mu}_t) q(\boldsymbol{\lambda}_t)} \\ q(\boldsymbol{\mu}_t^k) \propto \exp\langle \log\ p(\boldsymbol{z}_{1:t}^k, \boldsymbol{\alpha}_t)\rangle_{q(\boldsymbol{x}_t) q(\boldsymbol{\lambda}_t)} \\ q(\boldsymbol{\lambda}_t^k) \propto \exp\langle \log\ p(\boldsymbol{z}_{1:t}^k, \boldsymbol{\alpha}_t)\rangle_{q(\boldsymbol{x}_t) q(\boldsymbol{\mu}_t)} \end{cases}. \tag{8}$$

where $\langle\cdot\rangle_q$ denotes the expectation operator relative to the distribution q. Therefore, through a simple integral with respect to $\boldsymbol{\mu}_{t-1}^k$, the $a\ posteriori$ distribution $p(\boldsymbol{\alpha}_t^k|\boldsymbol{z}_{1:t}^k)$ can be sequentially updated. Considering the Eq. (3), the evolution of $\boldsymbol{\mu}_t^k$ is Gaussian, namely $p(\boldsymbol{\mu}_t^k|\boldsymbol{\mu}_{t-1}^k) \sim \mathcal{N}(\boldsymbol{\mu}_{t-1}^k, \bar{\boldsymbol{\lambda}}^k)$. Defining $q(\boldsymbol{\mu}_{t-1}^k) \sim \mathcal{N}(\boldsymbol{\mu}_{t-1}^{k*}, \boldsymbol{\lambda}_{t-1}^{k*})$, $q_p(\boldsymbol{\mu}_t^k)$ is also Gaussian, with the following parameters,

$$\begin{aligned} q_p(\boldsymbol{\mu}_t^k) &\sim \mathcal{N}(\boldsymbol{\mu}_{t\,p}^k, \boldsymbol{\lambda}_{t\,p}^k), \\ \text{where} \quad \boldsymbol{\mu}_{t\,p}^k = \boldsymbol{\mu}_{t-1}^{k*} \quad &\text{and} \quad \boldsymbol{\lambda}_{t\,p}^k = ({\boldsymbol{\lambda}_{t-1}^{k*}}^{-1} + (\bar{\boldsymbol{\lambda}}^k)^{-1})^{-1}. \end{aligned} \tag{9}$$

According to equation (8) and taking into account (7) and (9), variational calculus leads to closed-form expressions of $q(\boldsymbol{\mu}_t^k)$ and $q(\boldsymbol{\lambda}_t^k)$:

$$\begin{cases} q(\boldsymbol{\mu}_t^k) \sim \mathcal{N}(\boldsymbol{\mu}_t^{k*}, \boldsymbol{\lambda}_t^{k*}) \\ q(\boldsymbol{\lambda}_t^k) \sim \mathcal{W}_d(\boldsymbol{V}_t^{k*}, n^{k*}) \end{cases},$$

where the parameters are iteratively updated until convergence, according to the following scheme:

$$\begin{cases} \boldsymbol{\mu}_t^{k*} &= {\boldsymbol{\lambda}_t^{k*}}^{-1} (\langle\boldsymbol{\lambda}_t^k\rangle\langle\boldsymbol{x}_t^k\rangle + \boldsymbol{\lambda}_{t\,p}^k \boldsymbol{\mu}_{t\,p}^k) \\ \boldsymbol{\lambda}_t^{k*} &= \langle\boldsymbol{\lambda}_t^k\rangle + \boldsymbol{\lambda}_{t\,p}^k \\ n^{k*} &= \bar{n}^k + 1 \\ \boldsymbol{V}_t^{k*} &= (\langle\boldsymbol{x}_t^k {\boldsymbol{x}_t^k}^T\rangle - \langle\boldsymbol{x}_t^k\rangle\langle\boldsymbol{\mu}_t^k\rangle^T - \langle\boldsymbol{\mu}_t^k\rangle\langle\boldsymbol{x}_t^k\rangle^T \\ &\quad + \langle\boldsymbol{\mu}_t^k {\boldsymbol{\mu}_t^k}^T\rangle + (\bar{\boldsymbol{V}}^k)^{-1})^{-1} \end{cases}. \tag{10}$$

The mean state and the precision matrix distributions $q(\boldsymbol{\mu}_t^k)$ and $q(\boldsymbol{\lambda}_t^k)$ have closed forms, such that their expectations are easily derived:

$$\begin{cases} \langle\boldsymbol{\mu}_t^k\rangle &= \boldsymbol{\mu}_t^{k*} \\ \langle\boldsymbol{\mu}_t^k {\boldsymbol{\mu}_t^k}^T\rangle &= {\boldsymbol{\lambda}_t^{k*}}^{-1} + \boldsymbol{\mu}_t^{k*} {\boldsymbol{\mu}_t^{k*}}^T \\ \langle\boldsymbol{\lambda}_t^k\rangle &= n^{k*} \boldsymbol{V}_t^{k*} \end{cases}. \tag{11}$$

However, the state $\boldsymbol{x}_t^k$ to be estimated does not have closed form. Combining equations (7) and (8), $q(\boldsymbol{x}_t^k)$ has the following expressions:

$$q(\boldsymbol{x}_t^k) \propto \mathcal{N}(\langle\boldsymbol{\mu}_t^k\rangle, \langle\boldsymbol{\lambda}_t^k\rangle) \exp\langle \log\ p(\boldsymbol{z}_t^k|\boldsymbol{x}_t^k)\rangle. \tag{12}$$

Therefore, the GSEM and the observation model are naturally incorporated to update $q(\boldsymbol{x}_t^k)$. The distribution form immediately suggests an Importance Sampling procedure, where samples $\boldsymbol{x}_t^{k,(j)}$ are drawn from the Gaussian distribution $\mathcal{N}(\langle\boldsymbol{\mu}_t^k\rangle, \langle\boldsymbol{\lambda}_t^k\rangle)$, and are weighted according to their likelihoods:

$$\boldsymbol{x}_t^{k,(j)} \sim \mathcal{N}(\langle\boldsymbol{\mu}_t^k\rangle, \langle\boldsymbol{\lambda}_t^k\rangle), \quad w_t^{k,(j)} \propto \prod_{i \neq k}^{K_t} p(z_t^{k,i}|\boldsymbol{x}_t^{k,(j)}). \tag{13}$$

The observation expectations relative to $q(\cdot)$ in (12), are approximated by the observation with respect to the particles, when computing the particle weights. Accordingly, the expectation relative to $q(\boldsymbol{x}_t^k)$ is approximated by the Monte Carlo method:

$$\langle\boldsymbol{x}_t^k\rangle = \sum_{j=1}^{N} w_t^{k,(j)} \boldsymbol{x}_t^{k,(j)}, \tag{14}$$

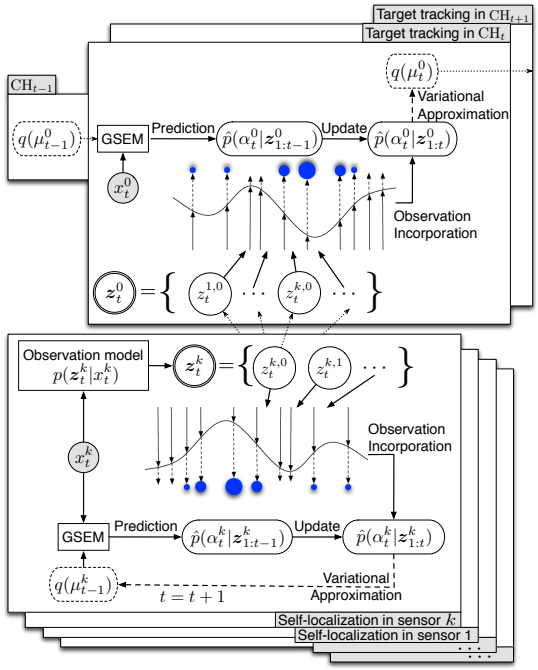

Fig. 2: Graphical illustration of the VF algorithm for CoSLAT in MANETs.

where N is the number of particles. Contrary to the traditional particle filtering (PF), the VF method reduces the temporal dependence from a huge amount of particles to a single Gaussian distribution $q(\boldsymbol{\mu}_{t-1}^k)$. To estimate the temporal positions of the mobile nodes, new particles are generated at each sampling instant, from the closed Gaussian distributions deduced from $q(\boldsymbol{\mu}_{t-1}^k)$ using variational calculus; and then they are sampled according to the temporal observations to calculate the corresponding expectations. We can tell from the procedure that the update phase and the approximation of the *a posteriori* distribution $p(\boldsymbol{\alpha}_t^k|\boldsymbol{z}_{1:t}^k)$ are jointly performed in the VF approach, yielding a natural and adaptive compression. Therefore, unlike other approximation method, e.g. the GMM in [8], the accumulation of approximation errors has been ended in the case of VF.

Besides the update of the *a posteriori* distribution introduced above, the predictive distribution $p(\boldsymbol{\alpha}_t^k|\boldsymbol{z}_{1:t-1}^k)$ can also be efficiently calculated using the VF approach:

$$\begin{aligned} \hat{p}(\boldsymbol{\alpha}_t^k|\boldsymbol{z}_{1:t-1}^k) &\propto \int p(\boldsymbol{\alpha}_t^k|\boldsymbol{\alpha}_{t-1}^k) q(\boldsymbol{\alpha}_{t-1}^k) d\boldsymbol{\alpha}_{t-1}^k \\ &\propto p(\boldsymbol{x}_t^k|\boldsymbol{\mu}_t^k, \boldsymbol{\lambda}_t^k) p(\boldsymbol{\lambda}_t^k) q_p(\boldsymbol{\mu}_t^k). \end{aligned} \quad (15)$$

The exponential form solution, which minimizes the Kullback-Leibler divergence between the predictive distribution and the separable approximate distribution $q_{t|t-1}(\boldsymbol{\alpha}_t^k)$, yields Gaussian distributions for the predicted expectations, and a

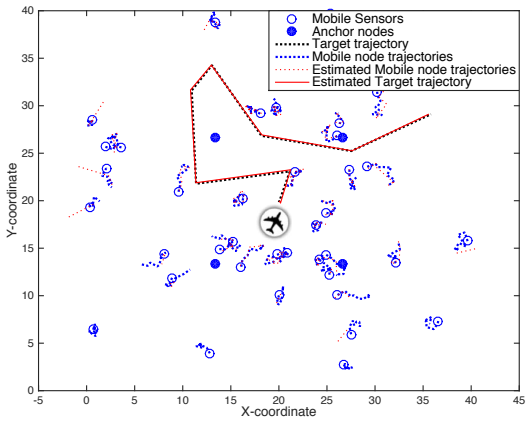

Fig. 3: Performance of the proposed algorithm after one trial.

Wishart distribution for the precision matrix:

$$\begin{cases} q_{t|t-1}(\boldsymbol{x}_t^k) \propto \mathcal{N}(\langle \boldsymbol{\mu}_t^k \rangle_{q_{t|t-1}}, \langle \boldsymbol{\lambda}_t^k \rangle_{q_{t|t-1}}) \\ q_{t|t-1}(\boldsymbol{\mu}_t^k) \propto \mathcal{N}(\boldsymbol{\mu}_{t|t-1}^{k*}, \boldsymbol{\lambda}_{t|t-1}^{k*}) \\ q_{t|t-1}(\boldsymbol{\lambda}_t^k) \propto \mathcal{W}_d(V_{t|t-1}^{k*}, n_{t|t-1}^{k*}) \end{cases}, \quad (16)$$

where the parameters are updated according to the same iterative schemes in Eq. (10) and (11). The state of the mobile node is then predicted by the following expressions:

$$\begin{aligned} \langle \boldsymbol{x}_t^k \rangle_{q_{t|t-1}} &= \langle \boldsymbol{\mu}_t^k \rangle_{q_{t|t-1}}, \\ \langle \boldsymbol{x}_t^k \boldsymbol{x}_t^{kT} \rangle_{q_{t|t-1}} &= \langle \boldsymbol{\lambda}_t^k \rangle_{q_{t|t-1}}^{-1} + \langle \boldsymbol{\mu}_t^k \rangle_{q_{t|t-1}} \langle \boldsymbol{\mu}_t^k \rangle_{q_{t|t-1}}^T. \end{aligned} \quad (17)$$

The computational cost and the memory requirements are dramatically reduced in the prediction phase compared to the PF method, because the predictive expectations have closed forms, avoiding the need of Monte Carlo integration.

Fig. 2 sums up the procedure of the VF algorithm for CoSLAT in MANETs.

4. NUMERICAL EXAMPLE

We consider a network of $N_a = 4$ anchors, $N_s = 40$ mobile sensors and one target moving freely within a field of size 40×40 m^2 as depicted in Fig. 3. Each sensor nodes has a sensing radius of $r_s = 15$ m, and a communication range of $r_c = 30$ m. In the simulations, we assumed a location prior that is uniform on the network field. However, due to the deployment error, mobile sensors are normally distributed around their initially setting locations with identical covariance matrix $\mathrm{diag}\{1, 1\}$. The mobile sensors and the target evolve independently according to the RWM model [10], as shown in Fig. 3. The observation noise variance is $\sigma^2 = 0.01$. The parameters involved in the GSEM were set as $\bar{\boldsymbol{\lambda}} = \mathrm{diag}\{1/10, 1/10\}$, $\bar{\boldsymbol{V}} = \mathrm{diag}\{1/10, 1/10\}$, $\bar{n} = 10$.

Performance of the proposed algorithm using $N = 100$ particles is shown in Fig. 3 and evaluated by Root Mean

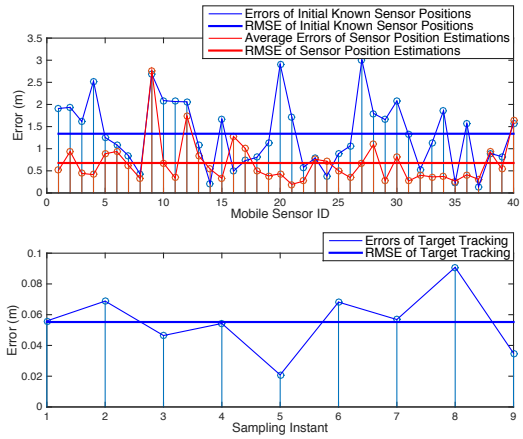

Fig. 4: Sensor localization and target tracking errors.

Square Error (RMSE) in Fig. 4. The average target tracking error is 0.0552 m, and the average sensor localization error is 0.6771 m against the initial deployment error of 1.3383 m. Therefore, in addition to the accurate tracking performance, remarkable refinements for sensor localization is demonstrated. However, since the algorithm is executed on a cluster base for energy efficiency, only the sensors that have detected the presence of the target are activated and re-located, which leads to precise localization of the sensors in high-traffic regions. On the contrary, sensors that are far from the target trajectory are left un-refined, corresponding to these unimproved localization errors in Fig. 4.

5. CONCLUSIONS

As the target moves freely in the MANET, a large number of measurements are generated, which facilitates both the activated sensors' localization and the target tracking. A distributed VF solution for CoSLAT is proposed in the context of MANETs, which interdependently and continuously improves the estimates of the mobile sensors and that of the target on-line, while reducing the resource consumption of the network. The improvement lies in the following characteristics: 1)the definition of the GSEM for the joint hidden state; 2) the variational calculus reduces the temporal dependence to only one single Gaussian statistic, which outperforms the classical PF algorithm in terms of inter-cluster communication; and 3) the update and the approximation of the $a\ posteriori$ distribution are jointly performed, allowing a lossless compression compared to other approximation methods.

References

[1] S. Farahmand, S.I. Roumeliotis, and G.B. Giannakis, "Set-membership constrained particle filter: Distributed adaptation for sensor networks," *IEEE Transactions on Signal Processing*, vol. 59, no. 9, pp. 4122–4138, September 2011.

[2] Isaac Amundson and Xenofon D. Koutsoukos, "A survey on localization for mobile wireless sensor networks," *Lecture Notes in Computer Science*, vol. 5801, pp. 235–254, 2009.

[3] Farah Mourad, Hichem Snoussi, Fahed Abdallah, and Cédric Richard, "Anchor-based localization via interval analysis for mobile ad-hoc sensor networks," *IEEE Transactions on Signal Processing*, vol. 57, no. 8, pp. 3226–3239, August 2009.

[4] Poonam Prasad, "Recent trend in wireless sensor network and its applications: a survey," *Sensor Review*, vol. 35, no. 2, 2015.

[5] Florian Meyer, Erwin Riegler, Ondrej Hlinka, and Franz Hlawatsch, "Simultaneous distributed sensor self-localization and target tracking using belief propagation and likelihood consensus," in *Conference Record of the Forty Sixth Asilomar Conference onSignals, Systems and Computers (ASILOMAR)*, Pacific Grove, CA, 4-7 Nov. 2012, pp. 1212–1216.

[6] Vladimir Savic and Henk Wymeersch, "Simultaneous localization and tracking via real-time nonparametric belief propagation," in *38th International Conference on Acoustics, Speech, and Signal Processing (ICASSP)*, May 2013, pp. 5180–5184.

[7] Christopher Taylor, Ali Rahimi, Jonathan Bachrach, Howard Shrobe, and Anthony Grue, "Simultaneous localization, calibration, and tracking in an ad hoc sensor network," in *Proceedings of the fifth international conference on Information processing in sensor networks*, 2006.

[8] Florian Meyer, Franz Hlawatsch, and Henk Wymeersch, "Cooperative simultaneous localization and tracking (coslat) with reduced complexity and communication," in *IEEE International Conference on Acoustics, Speech and Signal Processing (ICASSP)*. IEEE, May 26-31 2013, pp. 4484–4488.

[9] Jing Teng, Hichem Snoussi, Cédric Richard, and Rong Zhou, "Distributed variational filtering for simultaneous sensor localization and target tracking in wireless sensor networks," *IEEE Transactions on Vehicular Technology*, vol. 61, no. 5, pp. 2305–2318, June 2012.

[10] Tracy Camp, Jeff Boleng, and Vanessa Davies, "A survey of mobility models for ad hoc network research," *Wireless Communications and Mobile Computing*, vol. 2, pp. 483–502, 2002.